



Article

White Photoluminescence in Dy-Doped Oxyfluoride Glasses

Xianmei Chen ¹, Artemiy V. Khamenok ², Shaukat G. Khusainov ² , Mikhail V. Shestakov ^{2,*} 
and Victor V. Moshchalkov ³

¹ School of Physical Science and Technology, Southwest Jiaotong University, Chengdu 610031, China

² Department of Physics, Russian State Agrarian University-Moscow Timiryazev Agricultural Academy, Moscow 127434, Russia

³ Department of Physics and Astronomy, KU Leuven, BE-3001 Leuven, Belgium

* Correspondence: mvshestakov@rgau-msha.ru; Tel.: +7-499-976-21-89

Abstract: Dy³⁺-doped, Ag and Dy³⁺-co-doped, and Tm³⁺ and Dy³⁺-co-doped oxyfluoride glasses have been prepared by a conventional melt-quenching method. White and yellowish light emissions were generated in the glasses under excitation in the range from 350 to 390 nm. Changes in the excitation wavelength in the ultraviolet (UV) range do not significantly alter the emission tint of the Dy and Ag and Dy-co-doped glasses. On the contrary, the tint of the Tm and Dy co-doped glasses considerably varies under excitation in the same range.

Keywords: lanthanides; silver; oxyfluoride glass; photoluminescence; white light

1. Introduction

Lanthanide-doped compounds have been proposed for use in a number of such optical applications as optical thermometry [1], lasers [2], white light sources [3,4], nanoscintillators [5], bioimaging [6], and optical encoding [7]. Such a wide range of applications arose due to the versatile nature of the f-f optical transitions occurring in the lanthanide ions resulting in effective luminescence bands covering the whole visible range. Dy ions are especially promising for white light generation as they exhibit adjustable blue, yellow and red photoluminescence bands leading to a variable emission tint. Moreover, it is sufficient to dope a host solely with Dy³⁺ ions to generate white light effectively. So far, glassy, ceramic and glass-ceramic hosts suitable for doping with Dy have been proposed [4,8–12].

White light sources are essential in daily life due to their vast use for outdoor lighting [13–15]. White Light Emitting Diodes (WLED) were reported as the most promising technology for white light generation and replacement for incandescent and fluorescent lamps due to their remarkably high efficacy. The majority of commercial WLED is based on a phosphor-converted approach combining blue or near-UV LED excitation with conventional phosphor yellow or white light emission, respectively. Near-UV sources exhibit high electrical-to-optical-power conversion, independence of WLED emission spectrum on spectral shifts of excitation LED, a high color rendering index and a warm color temperature compared to the sources with blue excitation. In particular, the 365 nm excitation LEDs are the most appropriate due to their commercial availability.

An oxyfluoride glass host occupies a prominent position because of the low phonon energy environment for lanthanide ions and high transparency in near-UV-Vis ranges [3]. For the glasses proposed in this work, the highest phonon energy, attributed to SiO₄ tetrahedra, is at about 800 cm^{−1}. This value allows for low non-radiative decay rates and enhances the quantum yield of white luminescence. Likewise, the oxyfluoride glasses exhibit high transparency in the near-UV range, resulting in minimal energy losses under excitation at commercial 365 nm.

In articles [16,17], simple glass hosts with compositions of SiO₂-PbF₂ or SiO₂-PbF₂-AlO_{1.5} have been proposed. These simple glass hosts demonstrate high glass stability



Citation: Chen, X.; Khamenok, A.V.; Khusainov, S.G.; Shestakov, M.V.; Moshchalkov, V.V. White Photoluminescence in Dy-Doped Oxyfluoride Glasses. *Optics* **2023**, *4*, 66–73. <https://doi.org/10.3390/opt4010006>

Academic Editor: Marco Gandolfi

Received: 14 November 2022

Revised: 21 December 2022

Accepted: 13 January 2023

Published: 17 January 2023



Copyright: © 2023 by the authors. Licensee MDPI, Basel, Switzerland. This article is an open access article distributed under the terms and conditions of the Creative Commons Attribution (CC BY) license (<https://creativecommons.org/licenses/by/4.0/>).

and the capability to dissolve lanthanide ions in low concentrations. At the same time, the glasses can be melted at as low temperatures as 1000 °C for 5 min, which makes them promising for large-scale production due to low energy consumption. Moreover, the luminescence spectra of Dy-doped oxyfluoride glasses can be significantly modified with the addition of silver nanoparticles [9,18] or other lanthanides [19].

Regarding glass preparation techniques, melt-quenching, and physical vapor deposition techniques employ the fast cooling of hot liquids and vapors, respectively, resulting in some stable solid amorphous materials at room temperature. The melt-quenching method is widely used in labs because of its simplicity and suitability for the preparation of inorganic [20–22] or hybrid glasses [23]. The technique is suitable for large-scale production and even lab-fiber drawings. Physical vapor deposition is a more complex technique requiring the use of vacuum systems and is widely used for preparing organic glasses [24,25] on various substrates. A broad range of silica glasses can be prepared via the sol-gel polymeric route followed with the soaking of xerogels in solution and annealing in a gas atmosphere [26,27]. Moreover, silica-alkaline glasses can be successfully doped with Ag or Cu nanoclusters through the ion-exchange method [4,28].

In this work, we report on preparing Dy³⁺-doped, Ag and Dy³⁺ co-doped, and Tm³⁺ and Dy³⁺ co-doped oxyfluoride glasses with simple tricomponent host composition melted at 1000 °C for 5 min and quenched at room temperature. The prepared glasses emitted white light under excitation in the wide range from 350 to 390 nm.

2. Materials and Methods

The glasses were prepared by the conventional melt-quenching method described in detail elsewhere [16,29,30]. Briefly, silica, alumina, silver nitrate, lead, and dysprosium fluorides puratronic-grade powders (Alfa Aesar, Thermo Fisher GmbH, Tewksbury, MA, USA) were batched (5 g) and melted in a platinum crucible at 1000 °C for 5 min in air. Afterward, the melts were poured into an aluminum mold or left in the crucible and cooled down to room temperature. The prepared glasses were quite fragile and cracked upon cooling down. Nevertheless, the resultant pieces of the glasses were collected and polished out for some optical measurements. The chemical composition of the host was 53(SiO₂):42.8–42.9(PbF₂):5(AlO_{1.5}), mole %. The dysprosium and silver were added as dysprosium (0.1 mole %) or thulium (0.1 mole %) fluoride and silver nitrate (1 weight %). The higher concentrations of dysprosium fluoride led to some visible precipitates in the glasses. However, higher silver nitrate concentrations did not result in any precipitate or visible opalescence. The steady-state photoluminescence and excitation spectra were recorded with an electron-multiplied charge-coupled device (CCD) camera attached to a lab spectrometer using a xenon arc lamp as an excitation source, as described elsewhere [3].

3. Results

Figure 1a shows room-temperature photoluminescence emissions and excitation spectra of Dy-doped oxyfluoride glass under excitation at 350 (28,571 cm^{−1}), 365 (27,397 cm^{−1}) and 390 (25,641 cm^{−1}) nm. The detected photoluminescence spectra did not depend on an excitation wavelength. The spectra contained three major bands and two minor bands in the visible and near-infrared ranges, respectively. The maxima of the four main bands were located at 486 (20,921 cm^{−1}, blue color), 575 (17,391 cm^{−1}, yellow color), and 665 (15,038 cm^{−1}, red color) nm. Two minor bands were out of the scope of the research as they did not contribute to the visible spectrum. The blue, yellow and red bands were associated with radiative transitions in Dy³⁺ ions [9,18]. The excitation spectra contained four excitation bands covering the range from 300 (33,333 cm^{−1}) to 410 (24,390 cm^{−1}) nm. The band maxima were located at 325 (30,769 cm^{−1}), 350 (28,571 cm^{−1}), 363 (27,548 cm^{−1}), 387 (25,840 cm^{−1}), and 423 (23,641 cm^{−1}) to excitation transition from ⁶H_{15/2} ground state level to highly excited [9,18].

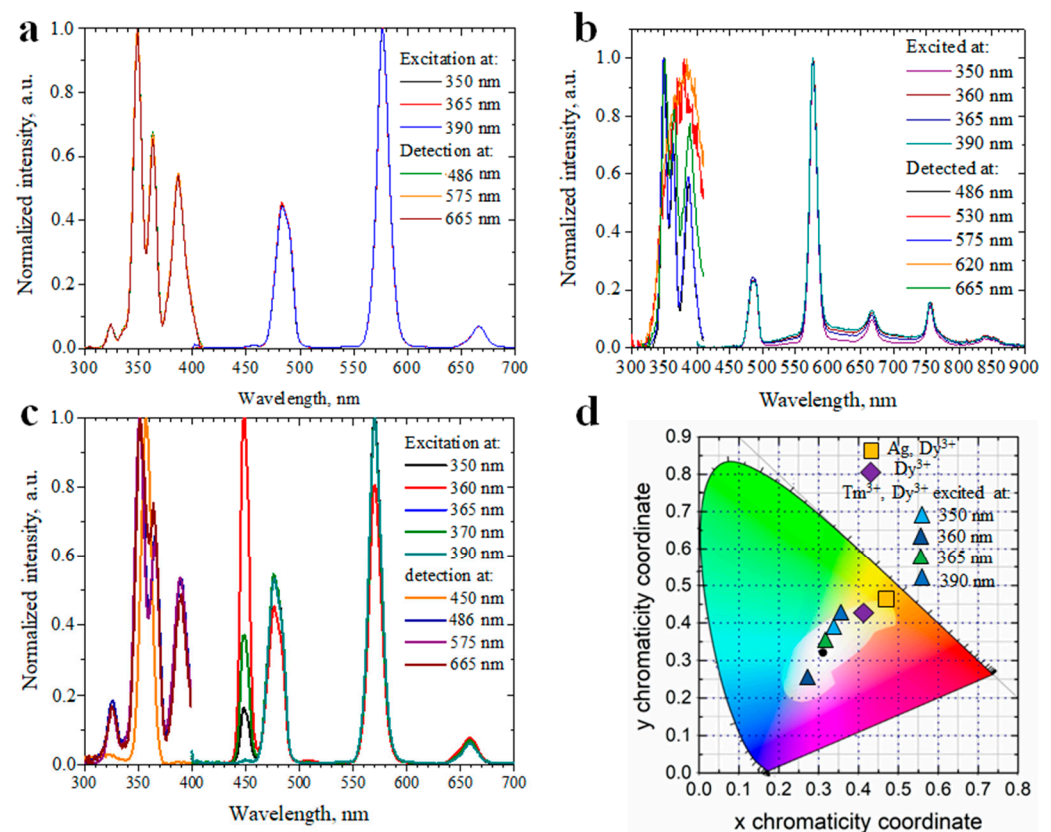


Figure 1. Room temperature steady-state photoluminescence and excitation spectrum of Dy-doped (a), Ag and Dy co-doped (b), and Tm and Dy co-doped (c) oxyfluoride glasses. Chromaticity CIE diagram (d) with emission color of the respective glasses at different excitation wavelengths.

Figure 1b shows the photoluminescence spectra of Ag and Dy³⁺-co-doped oxyfluoride glass excited in the range from 300 to 410 nm. The photoluminescence spectrum covers a broad range from 400 to 900 nm. In the spectrum, we see five prominent bands attributing to Dy³⁺ emission. The observed broad band, covering the whole range, corresponds to the earlier reported photoluminescence spectra of Ag-nanoclusters dispersed in oxyfluoride glasses [14,16]. The comprehensive research using Optical and Electron Spin Resonance Spectroscopy, Transmission Electron Microscopy and Time-Dependent Differential Functional Theory calculations showed that the rhombic Ag₄²⁺ nanoclusters were dispersed across fluorite lattice in the glass host giving quite similar broad emission in the respective range [14,16,31,32]. In the chemical composition of the glasses, lead fluoride constitutes 43 mole %. We believe that silver, being a highly mobile ion, homogeneously occupies all possible sites in the fluorite lattice that do not condense into large metallic droplets. The excitation spectra of Ag and Dy³⁺ co-doped oxyfluoride glass are shown in Figure 1b, exhibiting Dy³⁺ excitation bands detected at 486, 575 and 665, and Ag nanoclusters excitation bands detected at 530 (18,868 cm⁻¹) and 620 (16,129 cm⁻¹) nm. These detected excitation spectra conclude that Dy³⁺ ions and Ag nanoclusters were excited simultaneously and independently without any energy or electron transfers.

Figure 1c shows the photoluminescence excitation and emission spectra of Tm and Dy co-doped oxyfluoride glass. The emission spectrum contains three aforementioned Dy³⁺ emission bands and one Tm³⁺ emission band giving additional blue color to the emission. The Tm³⁺ emission band corresponds to the radiative transition between ¹D₂ and ³F₄ excited states [3]. The excitation spectra were detected at 450, 486, 575 and 665 nm. The former corresponds to the excitation of Tm³⁺ ions from the ³H₆ ground state to the ¹D₂ excited state. The latter three correspond to the aforementioned absorption transitions in Dy³⁺ ions.

The emission color of the prepared glasses is characterized by a CIE chromaticity diagram, where the (x, y) coordinates for each glass was calculated using the approach cited in [18]. The chromaticity coordinates and correlated color temperature (CCT) are summarized in Table 1. The CCT was calculated with the McCamy formula [33]. The CIE chromaticity diagram of Dy-doped, Ag and Dy co-doped, and Tm and Dy co-doped glasses are shown in Figure 1d. The black body point at 6667 K is placed at the center of the CIE diagram in the white light emission gamut. As seen from the figure, the Dy-doped glass (violet rhomb) and Ag and Dy co-doped glass (orange square) emit white and yellowish light, respectively, with small tint variation under excitation in the UV range. The emission color of Tm and Dy co-doped glass (colored triangles) significantly varies with a change of excitation wavelength covering almost the whole white gamut. The CCT values range from ~2900 to more than 10,000 K, favoring warm and cold emissions. Of note, there was no photobleaching of the glasses upon excitation with UV.

Table 1. The chromaticity coordinates and correlated color temperatures for the prepared glasses.

Glass Doped with	Excitation Wavelength, nm	Chromaticity Coordinate	CCT
Dy	350–390	(~0.41, ~0.43)	3676
Ag, Dy	350–390	(~0.47, ~0.46)	2918
Tm, Dy	350	(0.34, 0.38)	5238
Tm, Dy	360	(0.27, 0.25)	>10,000
Tm, Dy	365	(0.32, 0.35)	6035
Tm, Dy	390	(0.36, 0.42)	4745

4. Discussion

The energy level diagram of the Ag_n nanoclusters an Tm³⁺ and Dy³⁺ ions with the respective absorption and emission transitions are shown in Figure 2. The Ag_n energy level diagram depicts a series of nanoclusters with overlapping or quite close energies of the excited states. The ground (GS) and excited (ES1-3) state energies of the Ag_n nanoclusters were deduced from the experimental photoluminescence excitation and emission spectra. Upon excitation with UV, ES2 and ES3 levels get populated with electrons, followed by non-radiative de-excitation to the ES1 level. The ES1 level (hatched box) represents a number of the emitting excited states. The obtained excitation spectra were deconvoluted with a sum of two gaussian functions giving ES2 and ES3 excited levels with energies ~26,278 (381 nm) and ~29,923 (334 nm) cm⁻¹, respectively. This deconvolution indicates the presence of at least two different Ag_n nanoclusters in the glass host.

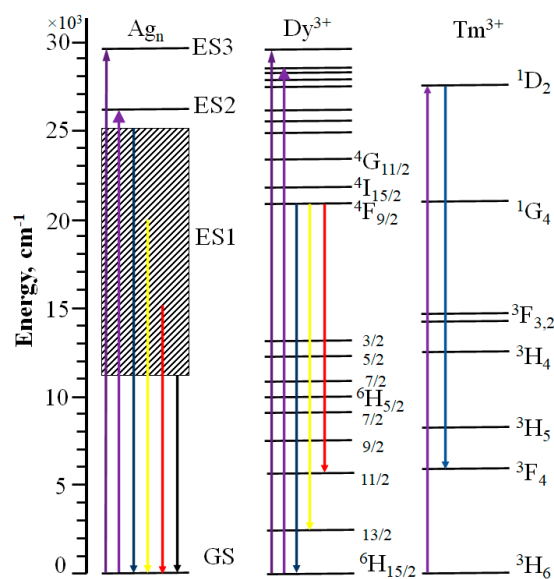


Figure 2. Energy level diagram of Ag nanoclusters (Ag_n), Dy³⁺ and Tm³⁺ ions.

The energy levels of Dy^{3+} and Tm^{3+} ions were taken from a Dieke diagram. Upon excitation with UV, highly excited levels of the Dy^{3+} ion (black and violet up-headed arrows) and the $^1\text{D}_2$ levels of Tm^{3+} ion (violet, up-headed arrow) became populated with electrons. The radiative transition from the $^1\text{D}_2$ to $^3\text{F}_4$ levels (blue, down-headed arrow) occurs, giving a blueish emission. The electrons from highly excited states of Dy^{3+} ions non-radiatively de-excited to $^4\text{F}_{9/2}$ followed by radiative transitions to $^6\text{H}_{11/2}$, $^6\text{H}_{13/2}$ and $^6\text{H}_{15/2}$ depicted with red, yellow, and blue down-headed arrows in Figure 2. As can be seen from the excitation spectra in Figure 1b,c, no energy transfer occurred between the Ag nanoclusters and Dy^{3+} ions and between the Dy^{3+} and Tm^{3+} ions, as reported in [19,34]. However, the small excitation band in the range from 300 to 340 nm in Figure 1c points out an energy transfer from the glass host to the Tm^{3+} ions. This band is not associated with the Dy^{3+} ions because of its maximum mismatch with Dy^{3+} excited levels and similar band observation in Tm^{3+} -doped oxyfluoride glasses [3].

Tm^{3+} ions are only effectively excited with wavelengths from 340 to 370 nm due to the strong optical absorption bringing the electrons from $^3\text{H}_6$ ground to $^1\text{D}_2$ excited level. At longer wavelengths, the excitation seems impossible, as we did not observe an efficient energy transfer from Dy high excited states to the $^1\text{D}_2$ state of Tm^{3+} ion accompanied with the de-excitation to $^1\text{G}_4$ excited state. The population of a $^1\text{G}_4$ -excited state with subsequent optical transitions might have brought about a photoluminescence emission band peaking around 450–475 nm [35–37]. However, the intensity ratios of the 575 and 486 nm peaks did not differ significantly upon excitation at 360 and 390 nm, corresponding to ~1.76 and ~1.89, respectively. This allows us to conclude that Tm^{3+} ion emission does not contribute to the 486 nm peak from the Dy ions due to its efficient multiple phonon non-radiative transition [38].

In this work, we prepared the glasses emitting white light with fixed and variable tints under excitation with UV light. Compared to our previous works [3,16,17], the glasses contained lanthanide ions in much lower concentrations. The quantum yield of the glasses was about 5% for excitation in the UV-blue ranges, as demonstrated by the measurements for similar glass compositions. The CCT covered a very wide range from ~3500 up to >10,000 K providing emissions suitable for various people's tastes. We did not expect good values of the color-rendering index (CRI) for solely the lanthanide-doped glasses compared to the Ag and Dy co-doped glasses, as those spectra did not cover the full visible range. However, the glasses still contained large amounts of lead, raising some concerns about their recyclability and environmental friendliness [39].

In the continuation of this work, we might consider the preparation of lead-free glass ceramics or ceramics containing low amounts of lanthanide ions with improved CRI for a white light generation [40,41]. Contemporary machine or deep-learning methods can facilitate our search for optimal chemical compositions [42,43].

5. Conclusions

Dy^{3+} -doped, Ag and Dy^{3+} -co-doped, and Tm^{3+} and Dy^{3+} co-doped oxyfluoride glasses have been prepared by conventional melt-quenching method at 1000 °C melted for 5 min in Pt crucible. The chemical composition of the oxyfluoride glass host was $\text{SiO}_2\text{-PbF}_2\text{-AlO}_{1.5}$. The prepared glasses emitted white light under excitation in the range from 300 to 410 nm with fixed and varied tint. The observed photoluminescence was associated with simultaneous independent excitation of Ag nanoclusters, Tm^{3+} and Dy^{3+} ions. A small band hinting energy transfer from the glass host to Tm^{3+} ions was observed. The glasses were found to be promising for outdoor lighting. In particular, the prepared glasses can be used as white-light-emitting layers combined with UV-emitting LEDs in the luminescent lamps. The main limitations of the prepared glasses are the high content of lead and low quantum yield. The former limitation can be resolved by substituting lead fluoride with lanthanum or yttrium fluoride. The latter could be resolved by dissolving silver and lanthanides in larger quantities in the glasses. Both limitations might require modifications

in the glass preparation method, as rare-earth fluoride dissolution is restricted in binary silica-lead fluoride glasses in high quantities under cooling.

Author Contributions: Conceptualization, X.C. and M.V.S.; investigation, X.C., M.V.S., and A.V.K.; resources, A.V.K.; discussion, S.G.K. and V.V.M.; writing—original draft preparation, X.C.; writing—review and editing, M.V.S. and S.G.K.; visualization, M.V.S.; supervision, S.G.K. and V.V.M.; project administration, M.V.S. and V.V.M.; funding acquisition, V.V.M. and M.V.S. All authors have read and agreed to the published version of the manuscript.

Funding: The experimental research was supported by the Methusalem funding from The Flemish Government. The data processing and analysis were funded with KU Leuven internal funds, Post-Doctoral Mandate PDM/16/108.

Data Availability Statement: The data presented in this study are available upon request from the corresponding author.

Conflicts of Interest: The authors declare no conflict of interest.

References

1. Dagupati, R.; Klement, R.; Rajavaram, R.; Velázquez, J.J.; Galusek, D. In Situ Synthesis of β -Na_{1.5}Y_{1.5}F₆:Er³⁺ Crystals in Oxyfluoride Silicate Glass for Temperature Sensors and Their Spectral Conversion and Optical Thermometry Analysis. *Molecules* **2021**, *26*, 6901. [\[CrossRef\]](#)
2. Kang, S.; Wang, W.; Qiu, J.; Yang, Z.; Dong, G. Intense Continuous-Wave Laser and Mode-Locked Pulse Operation from Yb³⁺-Doped Oxyfluoride Glass–Ceramic Fibers. *J. Am. Ceram. Soc.* **2022**, *105*, 5203–5212. [\[CrossRef\]](#)
3. Kuznetsov, A.S.; Nikitin, A.; Tikhomirov, V.K.; Shestakov, M.V.; Moshchalkov, V.V. Ultraviolet-Driven White Light Generation from Oxyfluoride Glass Co-Doped with Tm³⁺-Tb³⁺-Eu³⁺. *Appl. Phys. Lett.* **2013**, *102*, 161916. [\[CrossRef\]](#)
4. Yu, C.; Yang, Z.; Zhao, J.; Zhu, J.; Huang, A.; Qiu, J.; Song, Z.; Zhou, D. Luminescence Enhancement and White Light Generation of Eu³⁺ and Dy³⁺ Single-Doped and Co-Doped Tellurite Glasses by Ag Nanoparticles Based on Ag⁺-Na⁺ Ion-Exchange. *J. Alloy. Compd.* **2018**, *748*, 717–729. [\[CrossRef\]](#)
5. Bünzli, J.-C.G. Lanthanide-Doped Nanoscintillators. *Light. Sci. Appl.* **2022**, *11*, 285. [\[CrossRef\]](#) [\[PubMed\]](#)
6. Dong, H.; Du, S.-R.; Zheng, X.-Y.; Lyu, G.-M.; Sun, L.-D.; Li, L.-D.; Zhang, P.-Z.; Zhang, C.; Yan, C.-H. Lanthanide Nanoparticles: From Design toward Bioimaging and Therapy. *Chem. Rev.* **2015**, *115*, 10725–10815. [\[CrossRef\]](#) [\[PubMed\]](#)
7. Huang, K.; Idris, N.M.; Zhang, Y. Engineering of Lanthanide-Doped Upconversion Nanoparticles for Optical Encoding. *Small* **2016**, *12*, 836–852. [\[CrossRef\]](#)
8. Li, B.; Li, D.; Pun, E.Y.B.; Lin, H. Dy³⁺ Doped Tellurium-Borate Glass Phosphors for Laser-Driven White Illumination. *J. Lumin.* **2019**, *206*, 70–78. [\[CrossRef\]](#)
9. Vijayakumar, R.; Nagaraj, R.; Suthanthirakumar, P.; Karthikeyan, P.; Marimuthu, K. Silver (Ag) Nanoparticles Enhanced Luminescence Properties of Dy³⁺ Ions in Borotellurite Glasses for White Light Applications. *Spectrochim. Acta Part A Mol. Biomol. Spectrosc.* **2018**, *204*, 537–547. [\[CrossRef\]](#)
10. Xu, S.; Jia, F.; Zhang, G.; Zhao, T.; Zhang, H.; Su, C. Preparation and Luminescence Properties of Dy³⁺ Doped BaO-Al₂O₃-SiO₂ Glass Ceramics. *J. Non-Cryst. Solids* **2022**, *581*, 121436. [\[CrossRef\]](#)
11. Yan, Y.; Huo, H.; Zhang, H.; Zhao, T.; Wang, Q.; Zou, X.; Su, C. Preparation and Luminescence of Dy³⁺ Doped Glass-Ceramics Containing ZnMoO₄. *J. Non-Cryst. Solids* **2021**, *569*, 120990. [\[CrossRef\]](#)
12. Lin, C.; Wang, H.; Wang, P.; Wu, X.; Lin, T.; Sa, B.S.; Cheng, Y.; Zheng, X.; Yu, X.; Fang, C. Smart White Lighting and Multi-Mode Optical Modulations via Photochromism in Dy-Doped KNN-Based Transparent Ceramics. *J. Am. Ceram. Soc.* **2021**, *104*, 903–916. [\[CrossRef\]](#)
13. Ye, S.; Xiao, F.; Pan, Y.X.; Ma, Y.Y.; Zhang, Q.Y. Phosphors in Phosphor-Converted White Light-Emitting Diodes: Recent Advances in Materials, Techniques and Properties. *Mater. Sci. Eng. R Rep.* **2010**, *71*, 1–34. [\[CrossRef\]](#)
14. Kuznetsov, A.S.; Tikhomirov, V.K.; Shestakov, M.V.; Moshchalkov, V.V. Ag Nanocluster Functionalized Glasses for Efficient Photonic Conversion in Light Sources, Solar Cells and Flexible Screen Monitors. *Nanoscale* **2013**, *5*, 10065–10075. [\[CrossRef\]](#) [\[PubMed\]](#)
15. Wang, Y.; Zhu, G.; Xin, S.; Wang, Q.; Li, Y.; Wu, Q.; Wang, C.; Wang, X.; Ding, X.; Geng, W. Recent Development in Rare Earth Doped Phosphors for White Light Emitting Diodes. *J. Rare Earths* **2015**, *33*, 1–12. [\[CrossRef\]](#)
16. Shestakov, M.V.; Chen, X.M.; Kaydashev, V.; Baekelant, W.; Tikhomirov, V.K.; Vanacken, J.; Hofkens, J.; Moshchalkov, V.V. Oxyfluoride Glass (SiO₂-PbF₂) Co-Doped with Ag Nanoclusters and Tm³⁺ Ions for UV-Driven, Hg-Free, White Light Generation with a Tuneable Tint. *Opt. Mater. Express* **2014**, *4*, 1227. [\[CrossRef\]](#)
17. Shestakov, M.V.; Chen, X.; Baekelant, W.; Kuznetsov, A.S.; Tikhomirov, V.K.; Hofkens, J.; Moshchalkov, V.V. Lead Silicate Glass SiO₂-PbF₂ Doped with Luminescent Ag Nanoclusters of a Fixed Site. *RSC Adv.* **2014**, *4*, 20699–20703. [\[CrossRef\]](#)
18. Hua, C.; Shen, L.; Pun, E.Y.B.; Li, D.; Lin, H. Dy³⁺ Doped Tellurite Glasses Containing Silver Nanoparticles for Lighting Devices. *Opt. Mater.* **2018**, *78*, 72–81. [\[CrossRef\]](#)

19. Liu, X.; Chen, G.; Chen, Y.; Xu, J. Luminescent Properties and Energy Transfer of $\text{Tm}^{3+}/\text{Dy}^{3+}$ Co-Doped Oxyfluoride Borate Glasses for White LEDs. *J. Mater. Sci. Mater. Electron.* **2018**, *29*, 16041–16049. [[CrossRef](#)]
20. Niu, L.; Zhou, Y.; Zhu, C.; He, Z.; Meng, X. Pr^{3+} Doped Oxyfluoride Silicate Glasses for LEDs. *Ceram. Int.* **2019**, *45*, 4108–4112. [[CrossRef](#)]
21. Samir, A.; Hassan, M.A.; Abokhadra, A.; Soliman, L.I.; Elokr, M. Characterization of Borate Glasses Doped with Copper Oxide for Optical Application. *Opt. Quantum Electron.* **2019**, *51*, 123. [[CrossRef](#)]
22. Kolobkova, E.; Nikonorov, N.; Babkina, A.; Grabtchikov, A.; Khodasevich, I.; Korolkov, M. Concentration Dependence of Upconversion Luminescence of $\text{Er}^{3+}/\text{Yb}^{3+}$ in the Fluorophosphate Glasses with Small Phosphates Content. *Opt. Mater.* **2020**, *109*, 110279. [[CrossRef](#)]
23. Tao, H.; Bennett, T.D.; Yue, Y. Melt-Quenched Hybrid Glasses from Metal–Organic Frameworks. *Adv. Mater.* **2017**, *29*, 1601705. [[CrossRef](#)] [[PubMed](#)]
24. Tangpatjaroen, C.; Bagchi, K.; Martínez, R.A.; Grierson, D.; Szlufarska, I. Mechanical Properties of Structure-Tunable, Vapor-Deposited TPD Glass. *J. Phys. Chem. C* **2018**, *122*, 27775–27781. [[CrossRef](#)]
25. Kasting, B.J.; Beasley, M.S.; Guiseppi-Elie, A.; Richert, R.; Ediger, M.D. Relationship between Aged and Vapor-Deposited Organic Glasses: Secondary Relaxations in Methyl-m-Toluate. *J. Chem. Phys.* **2019**, *151*, 144502. [[CrossRef](#)] [[PubMed](#)]
26. El Hamzaoui, H.; Kinowski, C.; Razdobreev, I.; Cassez, A.; Bouwmans, G.; Prochet, B.; Capoen, B.; Bouazaoui, M. Synthesis, Structural and Optical Properties of Bismuth-Doped Sol-Gel-Derived Phosphosilicate Glasses. *Phys. Status Solidi (A) Appl. Mater. Sci.* **2019**, *216*, 1800411. [[CrossRef](#)]
27. El Hamzaoui, H.; Capoen, B.; Razdobreev, I.; Bouazaoui, M. In Situ Growth of Luminescent Silver Nanoclusters inside Bulk Sol-Gel Silica Glasses. *Mater. Res. Express* **2017**, *4*, 076201. [[CrossRef](#)]
28. Kumar, P.; Chandra Mathpal, M.; Hamad, S.; Rao, S.V.; Neethling, J.H.; Janse Van Vuuren, A.; Njoroge, E.G.; Kroon, R.E.; Roos, W.D.; Swart, H.C.; et al. Cu Nanoclusters in Ion Exchanged Soda-Lime Glass: Study of SPR and Nonlinear Optical Behavior for Photonics; Graphical Abstract Schematic Diagram Depicting Plasmonic Behavior of Cu NCs Embedded in Glass Matrix. *Appl. Mater. Today* **2019**, *15*, 323–334. [[CrossRef](#)]
29. Rodríguez, V.D.; Tikhomirov, V.K.; Velázquez, J.J.; Shestakov, M.V.; Moshchalkov, V.V. Visible-to-UV/Violet Upconversion Dynamics in Er^{3+} -Doped Oxyfluoride Nanoscale Glass Ceramics. *Adv. Opt. Mater.* **2013**, *1*, 747–752. [[CrossRef](#)]
30. Tikhomirov, V.K.; Rodríguez, V.D.; Kuznetsov, A.; Kirilenko, D.; van Tendeloo, G.; Moshchalkov, V.V. Preparation and Luminescence of Bulk Oxyfluoride Glasses Doped with Ag Nanoclusters. *Opt. Express* **2010**, *18*, 22032. [[CrossRef](#)]
31. Cuong, N.T.; Tikhomirov, V.K.; Chibotaru, L.F.; Stesmans, A.; Rodríguez, V.D.; Nguyen, M.T.; Moshchalkov, V.V. Experiment and Theoretical Modeling of the Luminescence of Silver Nanoclusters Dispersed in Oxyfluoride Glass. *J. Chem. Phys.* **2012**, *136*, 174108. [[CrossRef](#)] [[PubMed](#)]
32. Velázquez, J.J.; Tikhomirov, V.K.; Chibotaru, L.F.; Cuong, N.T.; Kuznetsov, A.S.; Rodríguez, V.D.; Nguyen, M.T.; Moshchalkov, V.V. Energy Level Diagram and Kinetics of Luminescence of Ag Nanoclusters Dispersed in a Glass Host. *Opt. Express* **2012**, *20*, 13582. [[CrossRef](#)] [[PubMed](#)]
33. Li, C.; Cui, G.; Melgosa, M.; Ruan, X.; Zhang, Y.; Ma, L.; Xiao, K.; Luo, M.R. Accurate Method for Computing Correlated Color Temperature. *Opt. Express* **2016**, *24*, 14066. [[CrossRef](#)] [[PubMed](#)]
34. Wei, C.; Xu, D.; Yang, Z.; Jia, Y.; Li, X.; Sun, J. Luminescence and Energy Transfer of Tm^{3+} and Dy^{3+} Co-Doped $\text{Na}_3\text{ScSi}_2\text{O}_7$ Phosphors. *RSC Adv.* **2019**, *9*, 27817–27824. [[CrossRef](#)] [[PubMed](#)]
35. Xiong, P.; Peng, M. Visible to Near-Infrared Persistent Luminescence from Tm^{3+} -Doped Two-Dimensional Layered Perovskite Sr_2SnO_4 . *J. Mater. Chem. C Mater.* **2019**, *7*, 8303–8309. [[CrossRef](#)]
36. El-Maaref, A.A.; Wahab, E.A.A.; Shaaban, K.S.; Abdelawwad, M.; Koubisy, M.S.I.; Börcsök, J.; Yousef, E.S. Visible and Mid-Infrared Spectral Emissions and Radiative Rates Calculations of Tm^{3+} Doped BBLC Glass. *Spectrochim. Acta Part A Mol. Biomol. Spectrosc.* **2020**, *242*, 118774. [[CrossRef](#)] [[PubMed](#)]
37. Liu, Y.; Bao, Y.; Dong, X.; Shang, J.; Yang, Y.; Dong, B. The $^1\text{G}_4\text{--}^3\text{H}_6$ Electron Transition Process of Tm^{3+} Promoted by Nonmetallic Plasmon. *Mater. Res. Bull.* **2020**, *124*, 110729. [[CrossRef](#)]
38. Darshan, G.P.; Premkumar, H.B.; Nagabhushana, H.; Sharma, S.C.; Prashantha, S.C.; Nagaswarup, H.P.; Prasad, B.D. Blue Light Emitting Ceramic Nano-Pigments of Tm^{3+} Doped YAlO_3 : Applications in Latent Finger Print, Anti-Counterfeiting and Porcelain Stoneware. *Dye. Pigment.* **2016**, *131*, 268–281. [[CrossRef](#)]
39. Meena, V.; Mohan, D.L.; Jayanta, K.S.; Hiranmoy, D.; Ashok, K.P. Impact of Lead Contamination on Agroecosystem and Human Health. In *Lead in Plants and the Environment*; Gupta, D., Chatterjee, S., Walther, C., Eds.; Springer International Publishing: Cham, Switzerland, 2020; pp. 67–82, ISBN 978-3-030-21638-2.
40. Wu, L.; Wu, Y.; Fan, Y.; Sun, B.; Li, Q.; Yu, J. Photoluminescence Properties and Energy Transfers in the Novel LiYMgWO_6 : Dy^{3+} , Tm^{3+} . *ECS Adv.* **2022**, *1*, 025001. [[CrossRef](#)]
41. Xiao, J.; Wang, C.; Min, X.; Wu, X.; Liu, Y.; Huang, Z.; Fang, M. Multiple Energy Transfer in Luminescence-Tunable Single-Phased Phosphor NaGdTiO_4 : Tm^{3+} , Dy^{3+} , Sm^{3+} . *Nanomaterials* **2020**, *10*, 1249. [[CrossRef](#)]

-
42. Biroli, G. Machine Learning Glasses. *Nat. Phys.* **2020**, *16*, 373–374. [[CrossRef](#)]
 43. Ravinder, R.; Sridhara, K.H.; Bishnoi, S.; Grover, H.S.; Bauchy, M.; Jayadeva; Kodamana, H.; Krishnan, N.M.A. Deep Learning Aided Rational Design of Oxide Glasses. *Mater. Horiz.* **2020**, *7*, 1819–1827. [[CrossRef](#)]

Disclaimer/Publisher’s Note: The statements, opinions and data contained in all publications are solely those of the individual author(s) and contributor(s) and not of MDPI and/or the editor(s). MDPI and/or the editor(s) disclaim responsibility for any injury to people or property resulting from any ideas, methods, instructions or products referred to in the content.